IL NUOVO CIMENTO **42 C** (2019) 31
DOI 10.1393/ncc/i2019-19031-0

Colloquia: SoHe3 2018

Compressed sensing and Sequential Monte Carlo for solar hard X-ray imaging

A. M. Massone([1])([2]), F. Sciacchitano([1]), M. Piana([1])([2]) and A. Sorrentino([1])([2])

([1]) *Dipartimento di Matematica, Università di Genova - Genova, Italy*
([2]) *CNR-SPIN - Genova, Italy*

received 28 December 2018

Summary. — We describe two inversion methods for the reconstruction of hard X-ray solar images. The methods are tested against experimental visibilities recorded by the *Reuven Ramaty High Energy Solar Spectroscopic Imager (RHESSI)* and synthetic visibilities based on the design of the *Spectrometer/Telescope for Imaging X-rays (STIX)*.

1. – Introduction

The NASA *Reuven Ramaty High Energy Solar Spectroscopic Imager (RHESSI)* [1] and the ESA *Spectrometer/Telescope for Imaging X-rays (STIX)* [2] are two space telescopes for imaging hard X-rays that rely on rather similar imaging technologies. *RHESSI* has been decommissioned on August 16 2018 after more than 16 years of successful operations, while *STIX* is going to fly in the next two years. Both hardwares allow the modulation of the X-ray flux coming from the Sun, providing as a result sparse samples of its Fourier transform, named visibilities, picked up at specific (u, v) points of the Fourier plane. Therefore, for both *RHESSI* and *STIX*, image reconstruction is needed to determine the actual spatial photon flux distribution from the few Fourier components acquired by the hard X-ray collimators [3-8]. In Section 2 of this paper we briefly overview a reconstruction method based on compressed sensing [9]. In Sec. 3 we provide more insights on a Monte Carlo method for the Bayesian estimation of several imaging parameters [10, 11]. Our conclusions are offered in Sec. 4.

2. – Compressed sensing for hard X-ray image reconstruction

Figure 1 shows how *RHESSI* and *STIX* grids sample the (u, v) frequency domain. From this design, it follows that the mathematical model for data formation in the

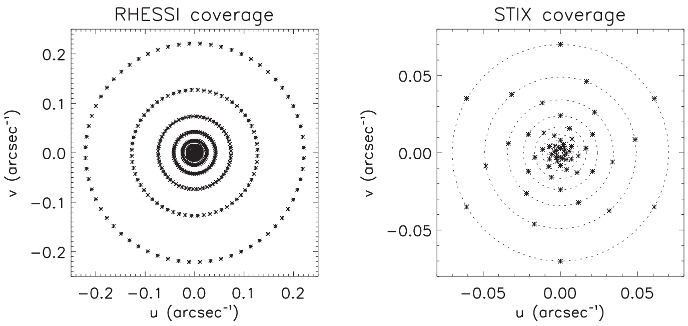

Fig. 1. – Sampling of the visibility (u, v) plane performed by *RHESSI* (left panel) and *STIX* (right panel), respectively.

framework of these two instruments is, in a matrix form:

$$HFx = V \ , \qquad (1)$$

where x is the photon flux image to reconstruct, V are the experimental visibilities, F is the discretized Fourier transform, H is a mask that realizes the sampling in the (u, v) plane. The reconstruction of x from V is an ill-posed problem and therefore regularization is required to mitigate the numerical instabilities induced by the observation noise. A possible approach is to apply an l_1 penalty term in some transformation domain. This can be realized by solving the minimum problem [9]

$$\hat{x} = \min_x \{\|HFx - V\|_2^2 + \lambda \|Wx\|_1\} \ , \qquad (2)$$

where the regularization term $\|Wx\|_1$ is designed to penalize reconstructions that would not exhibit the sparsity property with respect to the Finite Isotropic Wavelet Transform [9]. Figure 2 compares the reconstructions provided by this compressed sensing algorithm to the ones obtained by using other four visibility-based imaging methods currently implemented in the *RHESSI* pipeline [5-7].

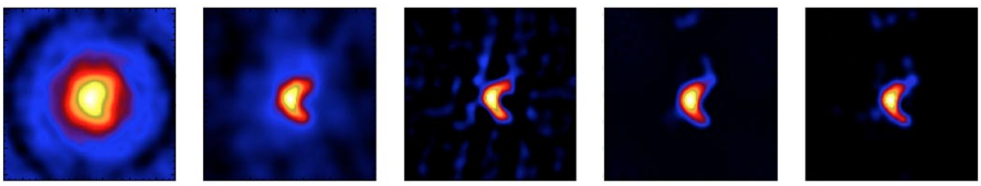

Fig. 2. – Image reconstructions from *RHESSI* visibilities provided, from left to right, by a Back-Projection algorithm, CLEAN, an interpolation/extrapolation method, a compressed sensing method based on exploiting an image catalogue, and by our wavelet-based compressed sensing method. The reconstructions refer to the May 13, 2013 event in the time interval 02:04:16-02:04:48 UT and energy range 6-12 keV. *RHESSI* visibilities recorded by detectors from 3 to 9 have been used in all cases.

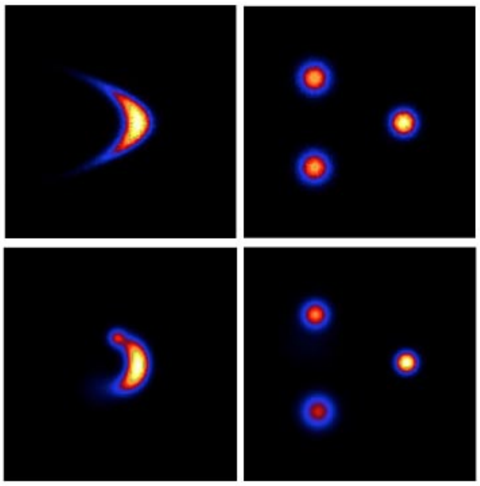

Fig. 3. – Reconstructions of two simulated configurations estimated by the SMC algorithm using synthetic *STIX* visibilities corresponding to a realistic signal-to-noise ratio. Top row: ground truth; bottom row: SMC reconstructions.

3. – Sequential Monte Carlo for hard X-ray image reconstruction

Sequential Monte Carlo (SMC) samplers are computational methods aiming at sampling target distributions of interest, and are often applied to sample the posterior distribution $p(x|y)$ as given by Bayes' theorem

$$p(x|y) = \frac{p(y|x)p(x)}{p(y)} \ , \tag{3}$$

where x is the unknown, y is the observation, $p(x)$ is the prior probability encoding all *a priori* information, $p(y|x)$ is the likelihood encoding the image formation model (1) and the noise model, and the marginal likelihood $p(y)$ is a normalization factor. In the case of *RHESSI* and *STIX* imaging, x is the image to reconstruct and y denotes the set of recorded visibilities. We modeled x as $x(N, T_{1:N}, \Theta_{1:N})$ where N is the number of sources in the image, $T_{1:N} = (T_1, \dots, N)$ represents the source types (Gaussian, elliptical, loop-like) and $\Theta_{1:N} = (\theta_1, \dots, \theta_N)$ contains the parameters characterizing each source. We chose a prior distribution factorized as the product of a Poisson distribution for N, uniform distributions for the source types and uniform distributions for the source parameters [10, 11]. Sequential Monte Carlo [12] computes the posterior distribution iteratively, by constructing a sequence of converging approximate distributions. Once the posterior is determined, it can be used to compute the solution image and all image parameters. Figures 3 and 4 show results provided by this approach using simulated *STIX* visibilities and experimental *RHESSI* visibilities, respectively.

4. – Conclusions

This paper shows the performances of two image reconstruction methods formulated for hard X-ray solar visibilities. The implementation of the corresponding tools within *Solar SoftWare (SSW)* is under construction.

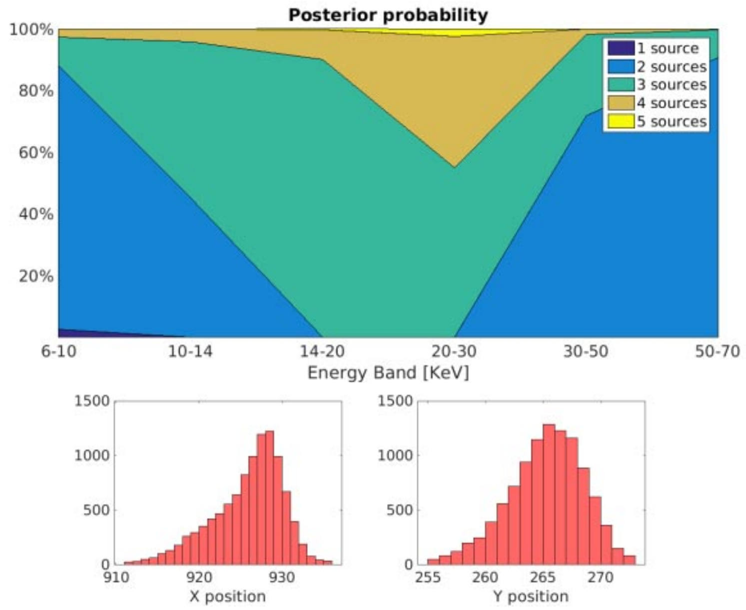

Fig. 4. – Parameters estimation provided by SMC in the case of the February 20, 2002 *RHESSI* visibilities. Top panel: posterior probabilities for the number of sources at different energy channels. Bottom panel: histograms of the x and y position of the loop-top source detected with high probability at the $20-30$ keV channel.

REFERENCES

[1] LIN, R. P. *et al.*, *Sol. Phys.*, **210** (3) 2002.
[2] BENZ, A. O. *et al.*, *The Spectrometer Telescope for Imaging X-rays on board the Solar Orbiter mission*, in *Space Telescopes and Instrumentation 2012: Ultraviolet to Gamma Ray*, edited by INTERNATIONAL SOCIETY FOR OPTICS AND PHOTONICS 2012, p. 84433L.
[3] ASCHWANDEN, M. J., BROWN J. C. and KONTAR E. P., *Sol. Phys.*, **210** (383) 2002.
[4] BENVENUTO, F., SCHWARTZ R., PIANA M. and MASSONE A. M., *Astron. Astrophys.*, **555** (A61) 2013.
[5] DENNIS, B. R. and PERNAK R. L., *Astrophys. J.*, **698** (2131) 2009.
[6] FELIX, S., BOLZERN R. and BATTAGLIA M., *Astrophys. J.*, **849** (10) 2017.
[7] MASSONE A. M., EMSLIE A. G., HURFORD G. J., PRATO M., KONTAR E. P. and PIANA M., *Astrophys. J.*, **703** (2004) 2009
[8] METCALF T. R., HUDSON H. S., KOSUGI T., PUETTER R. C. and PINA R. K., *Astrophys. J.*, **466** (585) 1996.
[9] DUVAL POO M., PIANA M. and MASSONE A. M., *Astron. Astrophys.*, **615** (A59) 2018.
[10] SCIACCHITANO F., LUGARO S. and SORRENTINO A., *SIAM J. Imag. Sci., accepted,* (arXiv preprint:1807.11287) .
[11] SCIACCHITANO F., SORRENTINO A., EMSLIE A. G., MASSONE A. M. and PIANA M., *Astrophys. J.*, **862** (68) 2018.
[12] DEL MORAL P., DOUCET A. and JASRA A., *J. R. Stat. Soc. B*, **68** (411) 2006.